ESTIMATING NORTH PACIFIC SUMMER SEA-LEVEL PRESSURE BACK TO 1600 USING PROXY CLIMATE RECORDS FROM CHINA AND NORTH AMERICA

Wu Xiangding (吴祥定)

Institute of Geography, Academia Sinica, Beijing

and *J. M. Lough*

Laboratory of Tree-Ring Research, University of Arizona, Tucson, AZ 85719, U.S.A.

Received October 31, 1985

ABSTRACT

Sea-level pressure variations over the North Pacific Ocean influence the surface climate conditions of China and western North America. Documentary records of precipitation in China data back to the mid-15th century, and a well-replicated network of tree-ring chronologies from western North America dates to the early 17th century. These proxy climate records are used separately and together to estimate sea-level pressure variations over the North Pacific back to 1600 A.D. The models are calibrated over the period 1899 to 1950 and verified over the independent period, 1951 to 1963. The best estimates, derived from predictors in China and western North America, calibrate 44.7% of summer sea-level pressure variance. The study demonstrates the potential of combining different proxy data sources to derive estimates of past climate.

I. INTRODUCTION

Proxy series are the only source of climatic information prior to the widespread introduction of instrumental measurements. Each proxy climate series is likely to contain error and biases unrelated to climate. It is, therefore, thought that the most realistic picture of past climate can be achieved only by the comparison and integration of different proxy sources (NAS, 1975). In this study we use documentary records and tree-ring chronologies both separately and together to estimate past sea-level pressure variations over the North Pacific.

Dendroclimatology involves the estimation of past climate variations from the annual ring-width variations of trees (Fritts, 1976; Hughes et al., 1982). A spatial array of 65 western North American tree-ring chronologies has been used to estimate spatial patterns of past climate (Fritts et al., 1979). Seasonal estimates of sea-level pressure at 96 grid points over the North Pacific and North America were developed from these tree-ring chronologies for the period 1602 to 1961.

The Central Meteorological Bureau (1981) of China has assembled and analyzed a variety of historical information from China to produce yearly wetness and dryness indices for 120 sites for the period 1470 to 1979. These precipitation indices refer primarily to the intensity of the summer monsoon (Wang and Zhao, 1981).

The basis for this study is that tree growth in western North America and precipitation in China are both influenced by the large-scale atmospheric circulation over the North Pacific. We first calibrate and estimate summer season sea-level pressure for 56 grid points in the North Pacific directly from the documentary precipitation indices. These estimates are then compared

to those derived from western North American tree-ring chronologies. Finally, estimates are derived using both the Chinese and western North American proxy series as predictors.

II. DATA

1. *Chinese Data*

Although the Chinese precipitation indices are for up to 120 sites, there are considerable variations in the number of sites with assigned index values in any given year. We, therefore, selected a subset of 44 sites with 10% or fewer missing years in the period 1600 to 1979. The year 1600 was chosen as the initial year of this series because it is the first year of the North American tree-ring chronologies. The 44 sites (Fig. 1) are located east of 105°E and south of 40°N, i.e. in the eastern region of China. The rainfall indices consist of five grades: 1 = very wet, 2 = wet, 3 = normal, 4 = dry and 5 = very dry. Missing values for the selected 44 sites were replaced by the value 3, for normal.

To reduce the size of this 44-site data set for the model calibration procedures, principal component analysis using the correlation matrix was performed for the period 1600 to 1979. The amplitudes of the first ten eigenvectors, explaining 63% of the total variance (referred to as the CH44RF set), were retained for model development. Statistical testing demonstrated that these amplitudes were all normally distributed.

2. *Tree-Ring Data*

Two North American tree-ring predictor sets were used. Both were based on the 65 west-

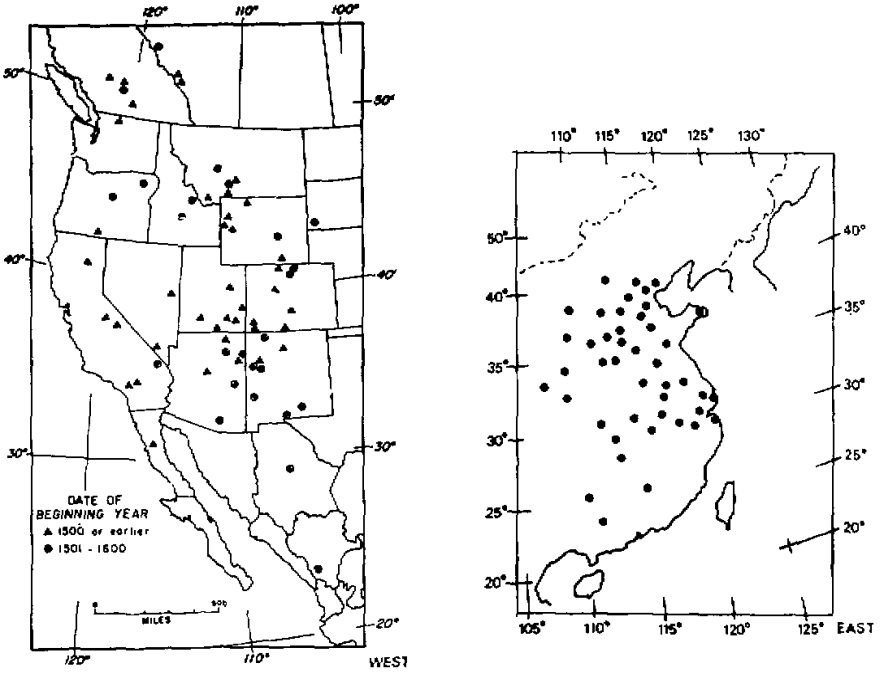

Fig. 1. Location of 44 Chinese precipitation index sites (right) and 65 western North American tree-ring chronology sites (left).

ern North American chronology grid (Fritts and Shatz, 1975 and Fig. 1) used previously to develop spatial reconstructions of climate (Fritts et al., 1979). What we shall refer to as the I65TR set are the amplitudes of the first 15 eigenvectors of the original chronologies which explain 69% of the total variance. The R65TR set are the amplitudes of the first 15 eigenvectors of the same data after autoregressive–moving average (ARMA) modeling (see Rose, 1983). These explain 68% of the total variance. The first of these data sets covers the period 1600 to 1963, and the second, 1601 to 1963.

We would not expect a high correlation between these tree–ring data sets and summer sea–level pressure because the ring widths reflect the integrated effects of growth in all seasons (Fritts, 1976; Fritts and Lough, in press). Large anomalies in climate during seasons other than summer would be likely to produce outliers in the reconstructed data. In spite of these potential drawbacks there is enough climatic information in the tree–ring data to warrant their use, in conjunction with the Chinese precipitation indices, to reconstruct summer sea-level pressure.

3. *Sea-Level Pressure Data*

Sea–level pressure data, for the summer season (June, July and August) were taken from the National Center for Atmospheric Research/Trenberth corrected set for the period 1899 to 1980 (Trenberth and Paolino, 1980). Preliminary analyses were performed using the entire 96–point grid (20 to 70°N, 100°E to 80°W), but this grid was found to be too large an area for model calibration. The Chinese precipitation indices have been shown (Lough et al., in preparation) to be most closely linked to sea–level pressure in the central and western portions of the North Pacific. We, therefore, selected a smaller, 56–point grid array for further study covering the area 20 to 50°N/100°E to 130°W. (The grid points are located at 10–degree latitude intervals and 10–degree longitude intervals.) Principal component analysis of these data was performed using the covariance matrix over the period 1899 to 1980. The first five eigenvectors which explain 69.0% of the total variance form the predictand data set.

III. METHODS

The multivariate transfer function methods described by Fritts et al. (1979) and Lofgren and Hunt (1982) were used to calibrate the models. The predictands, as represented by the first five principal components of summer sea–level pressure, were calibrated with the predictors–the CH44RF, I65TR or R65TR data sets–using canonical regression techniques (Blasing, 1978). Once the best model was developed, multiplication by the fitst five eigenvectors of the sea–level pressure data produced estimates for each grid point and year.

Verification is an important aspect of statistical calibration models. Once a model is developed it is necessary to test the reliability of the resulting estimates with data independent of those used for model calibration. In developing the 96–point sea–level pressure reconstructions, Fritts et al. (1979) used all the available data in the calibration procedure over the period 1899 to 1962 and applied sub–sample replication techniques using data from within the calibration period to verify the general form, though not the estimates, of the final model (Gordon. 1982). In the present study we kept data aside from the calibration period for independent verification. Several different calibration and verification periods were tested. All the results presented here are based on the 1899 to 1950 calibration and 1951 to 1963 verification periods.

The success of a particular model calibration was determined first by the overall percentage variance calibrated and second by the model's performance over the independent verification

period. In assessing the results for the verification period we used the percentage of the total number of 56 grid points passing particular statistical tests. This procedure contrasts with that of Fritts et al. (1979) who verified the orthogonal principal components of sea-level pressure. The latter approach overcomes the problem of spatial correlation in the 56-point grid. The presence of collinearity in the sea-level pressure data set affects the critical percentage of tests one would expect to pass by chance (Livezey and Chen, 1983). From the binomial distribution we can calculate that if a finite number of 56 significance tests are performed, 11.2% or more must pass to guarantee at least 95% significance of the collective set (Livezey and Chen, 1983). Monte Carlo simulations of the calibration and verification procedures to assess the effect of spatial correlation on the collective significance of the results were beyond the scope of the project.

A number of statistics were considered in assessing the reliability of a particular model. For the model as a whole, the percentage variance calibrated (EV) was considered as well as the explained variance (EV*) adjusted for overestimation due to the number of predictors and observations used (Kutzbach and Guetter, 1980). The reliability of a particular model over the calibration and verification periods was assessed by the number of tests passed at the 95% confidence level of the following statistics: a) the correlation coefficient (r); (b) the correlation coefficient of the first differences (r first diff.); c) the sign test agreement; (d) the sign test agreement of the first differences; e) the product mean tests; and f) the percentage of all tests significant. In addition, the number of grid points with positive reduction of error (RE) values, indicating some model skill, was computed for the verification period.

Our analyses differ from those of Fritts et al. (1979) in three other major respects. First, we use June, July, August as the summer season-this is not, therefore, directly comparable to their July and August season. Second, Fritts et al. (1979) used lagged predictors with first-order autocorrelation removed to deal with the autoregressive and moving average relationships between tree-rings and climate. We did not use any lagged predictors but did use the ARMA modeled western U.S. chronologies as well as the original data. Third, Fritts et al. (1979) found that a number of models of different structure produced reliable calibration and verification statistics. They, therefore, averaged the two best models to produce their final estimate of summer sea-level pressure back to 1602. We did not use any averaging procedures in this study.

IV. RESULTS

1. *Reconstruction Development*

The first calibration, using the first ten amplitudes of Chinese precipitation (CH44RF) as predictors is summarized in Table 1. Three of the five canonical variates passed the significance test at the 95% confidence level and the entire model calibrated 19.7% of the sea-level pressure variance with an adjusted calibrated variance of only 9.0%. The spatial distribution of the calibrated variance (Fig. 2, top) ranges from one to a maximum of 34%. The model explains most variance over the Chinese mainland and in the western sector of the North Pacific subtropical anticyclone. Over the verification period, 17.9% of the grid points have positive RE statistics though only 9.3% of all possible significance tests are passed. Greatest agreement between the instrumental and estimated data (17.9% of the total) is found in the correlation of the first differences, which measures the high-frequency information content. The spatial distribution of the number of tests passed and RE statistic (Fig. 2, bottom) shows

that the model has some skill only at the margins of the grid-areas where the calibrated variance is low.

Table 1. Summary of Calibration (1899 to 1950) and Verification (1951 to 1963) Results for Reconstructions of Summer Sea-Level Pressure

Model Statistics (%)	CH44RF	I65TR	R65TR	CH44RF + I65TR	CH44RF + R65TR
Calibration					
EV	19.7	34.1	26.0	54.5	44.7
EV*	9.0	13.8	10.5	25.1	21.7
r sig.	91.1	94.6	83.9	100.0	100.0
r first diff. sig.	85.7	92.9	73.2	100.0	94.6
Sign tests sig.	55.4	92.9	51.8	96.4	82.1
Sign tests first diff. sig.	48.2	53.6	41.1	85.7	60.7
Prod. mean tests sig.	64.3	75.0	67.9	92.9	83.9
All tests sig.	68.9	81.8	63.6	95.0	84.3
Varification					
r sig.	10.7	1.8	7.1	7.1	17.9
r first diff. sig.	17.9	3.6	8.9	3.6	19.6
Sign tests sig.	5.4	1.8	8.9	3.6	23.2
Sign tests first diff. sig.	8.9	1.8	1.8	3.6	8.9
Prod. mean tests sig.	3.6	0.0	7.1	1.8	1.8
All tests sig.	9.3	1.8	6.8	3.6	14.3
RE>0	17.9	1.8	41.1	8.9	46.4
Rank	3	4	5	2	1

In the second calibration, using the I65TR predictor set, four of the five canonical variates were passed, explaining 34.1% of the sea-level pressure variance, adjusted to 13.8%. Spatially (Fig. 3, top) the calibrated variance varies from less than zero to a maximum of 44.0%. Comparison with the CH44RF model (Fig. 2, top) shows that the areas of maximum explained variance are very similar for the two predictor sets from opposite sides of the Pacific. Both the models calibrate most variance in the vicinity of the North Pacific subtropical anticyclone and over the Chinese mainland, and show a minimum of calibrated variance in northeast China and over the Sea of Japan. Although this model (I65TR) calibrates more variance than the CH44 RF (Table 1), it performs less well over the verification period with only one grid point exhibiting a positive RE statistic and only 1.8% of the total number of tests passed (Fig. 3, bottom).

The third calibration, using the ARMA modeled 65 western north American chronologies, the R65TR predictor set, passed three of the five canonical variates and explains 26.0% of the variance, adjusted to 10.5%. This is less than that using the original (I65TR) chronologies but greater than the CH44RF calibration. The distribution of the calibrated variance (Fig. 4,

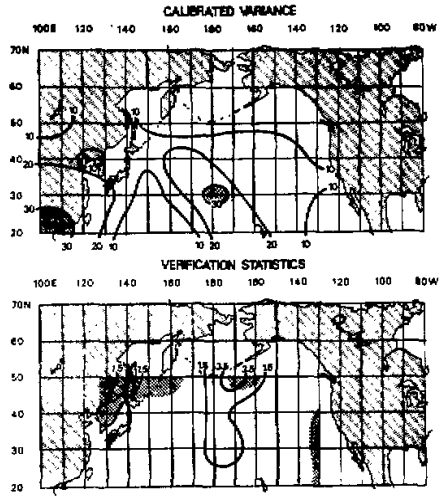

Fig. 2. Percentage of calibrated variance (top), number of tests passed (shaded) and RE values for verification period (bottom) for CH44RF model.

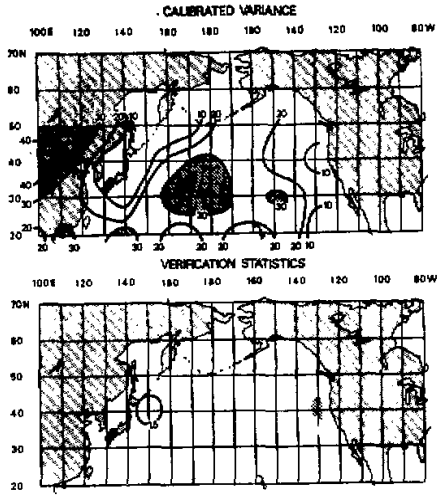

Fig. 3. As in Fig. 2 but for I65TR model.

top) shows that most variance, greater than 30%, is explained in the vicinity of the North Pacific subtropical anticyclone. Over the verification period, however, the R65TR predictors appear to perform better with 41.1% of the grid points having positive RE statistics. Verification is best in the southwestern and northwestern portions of the grid (Fig. 4, bottom). These regions of positive RE statistics do not appear in the areas of maximum calibrated variance. Despite the rather high percentage of positive RE statistics, only 6.8% of all tests were significant.

Summarizing the results at this stage we note that using the Chinese predictors alone, 19.7% variance is calibrated, and using the original 65 North American chronologies alone, 34.1% variance is calibrated. The ARMA-modeled North American chronologies explain 26.0% of the variance. Spatially, all three models calibrate most variance over China and in the western sector of the North Pacific subtropical anticyclone. Over the verification period, the ARMA-modeled North American chronologies show most skill with 41.1% of the grid points having positive RE statistics though the percentage of the other tests passed is still very low. The original North American chronologies appear to produce the least reliable estimates, having only one grid point with a positive RE value over the verification period.

Two final models were developed in which the predictors included both eastern Chinese and western North American information. The first of these models used the first ten Chinese precipitation amplitudes (CH44RF) and the first fifteen of the original (I65TR) North American chronology amplitudes. The second of these merged predictor sets used the first fifteen amplitudes of the ARMA modeled (R65TR) North American chronologies, together with the CH44RF set. The calibration and verification results are summarized in Table 1 and Figs.5 and 6.

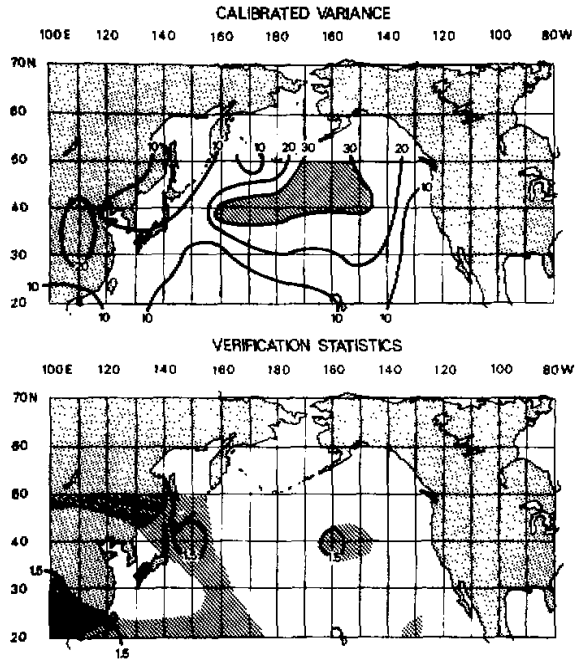

Fig. 4. As in Fig. 2 but for R65TR model. Calibrated variance (top) and verification statistics (bottom).

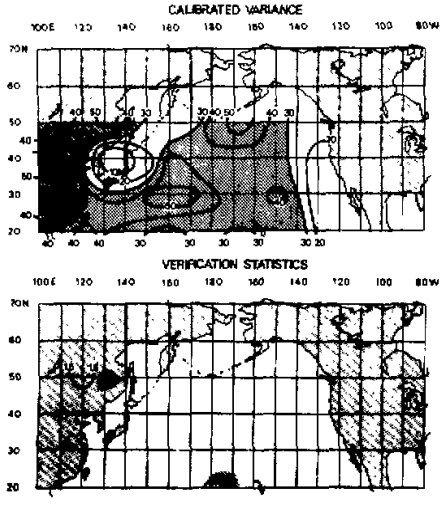

Fig. 5. As in Fig. 2 but for CH44RF+I65TR model.

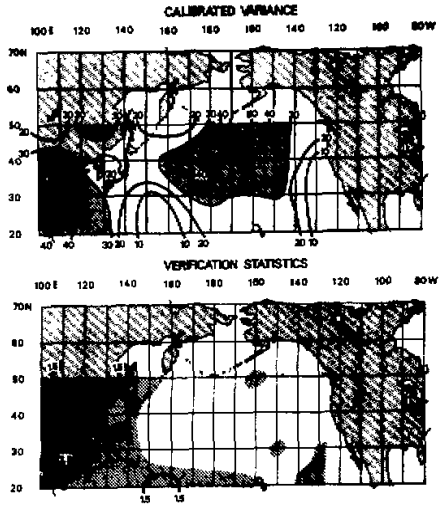

Fig. 6. As in Fig. 2 but for CH44RF+R65TR model.

The first of these merged models makes four of the five canonical variates pass at the 95% confidence level, and explains 54.5% of the variance—very close to the sum (53.8%) of the two

independent calibrations. Over the verification period, however, this merged model shows less skill than the CH44RF predictor set alone, with only 3.6% of all significance tests passed and 8.9% of grid points with positive RE statistics.

From the statistics summarized in Table 1 and their spatial distribution (Fig. 5, bottom) we conclude that this model shows no reliability over independent data above that is expected by chance. This result illustrates how high calibrated variance is not always a good indication of a model's performance.

The merged model based on the R65TR set, passed three of the five canonical variates and explained 44.7% of the variance, adjusted to 21.7%. Spatially, most variance is calibrated (greater than 30%) over the Chinese mainland and in the vicinity of the North Pacific subtropical anticyclone. This model performs better over the verification period than either the R65TR or CH44RF sets alone: 17.9% of the grid points exhibit significant correlation between the instrumental and estimated data and 16.3% of all tests are passed. In addition, 46.4% of the grid points have positive RE statistics. Spatially, however, these areas of significant verification are found only in the area of high calibrated variance over the Chinese mainland and verification is weak in the vicinity of the North Pacific subtropical anticyclone (Fig. 6, bottom).

By ranking the models in order for each of the statistics presented in Table 1, the best calibration of summer sea-level pressure appears to be that using the combined CH44RF+R65TR as predictors followed by the combined CH44RF+I65TR set. The use of the combined predictors from both sides of the North Pacific, therefore, appears to produce a more reliable reconstruction than any of the individual predictor sets. Although the improvement of the combined sets over the individual sets is not very large it does illustrate the potential of using mixed proxy data predictor sets to develop past climate reconstructions.

2. *Analysis of the Reconstructions*

In this short paper it is not possible to present all the yearly or even decadally averaged reconstructions of sea-level pressure. We, therefore, look at only some of the features of the reconstructions derived from the CH44RF+R65TR model: in the first subsection the average of the reconstructions over the independent period, 1600 to 1898, is compared to the instrumental record mean. We then look at the estimated sea-level pressure field for two individual years and two ten-year average periods.

(1) *Comparison with instrumental mean*

Fig. 7 shows, superimposed on the mean summer sea-level pressure field for the 20th century, the average reconstructed departure for the independent period 1601 to 1898. The average sea-level pressure prior to the 20th century is reconstructed to be higher over most of the grid with a maximum increase in the western sector of the North Pacific subtropical anticyclone. This suggests that on the average we are estimating a slightly intensified and/or westward displaced high pressure cell-the circulation feature which is strongly related to Chinese precipitation features (Lough et al., in preparation). Higher sea-level pressure is linked to wetter conditions and lower sea-level pressure to drier conditions in China.

The time series of PC1 amplitudes of the 44-site Chinese precipitation indices (not shown) represents the large-scale variations affecting most of eastern China. High positive values indicate drier conditions and low negative values, wetter conditions. When averaged over the whole period 1601 to 1898 the mean of the amplitudes is −0.14 (indication a slight tendency towards wetter conditions). This compares with a mean value of +0.36 over the

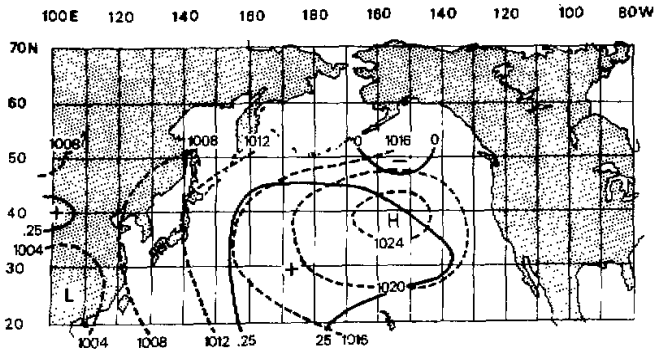

Fig. 7. Reconstructions from CH44RF+R65TR model, averaged for the period 1600 to 1899 (solid line) and compared to the mean of the instrumental record (broken line).

period 1899 to 1963, suggesting drier conditions on average. Although the difference between these two mean values is not statistically significant, the difference is consistent with the average reconstructed mean sea-level pressure departure for the two periods.

(2) *Yearly and Decadal Averages*

In this subsection we present maps for two individual years and two decades. These years were selected on the basis of very wet or very dry conditions in eastern China, as measured by the mean of the amplitude of the first principal component of the 44-site precipitation indices.

During the period 1601 to 1898, 1640 is the driest year and 1648 is the wettest year in

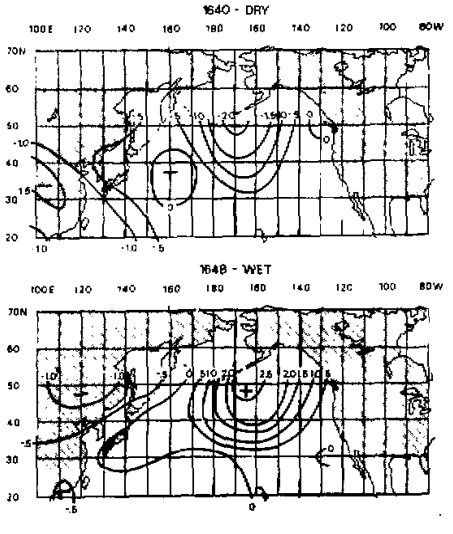

Fig. 8. Reconstructed summer sea-level pressure for 1640-DRY (top) and 1648-WET (bottom).

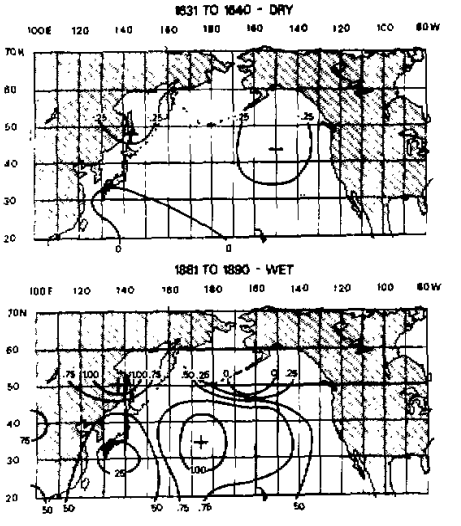

Fig. 9. Reconstructed summer sea-level pressure averaged for the decades 1631 to 1640-DRY (top) and 1881 to 1890-WET (bottom).

eastern China as represented by the component amplitude. In the estimated summer sea-level

pressure field for 1640 (Fig. 8, top), lower sea-level pressure is found in the vicinity of the North Pacific subtropical anticyclone, indicating a weakening of this circulation feature. Lower sea-level pressure is reconstructed over the Chinese mainland. The North Pacific subtropical anticyclone and Aleutian low are important controls on summer monsoon precipitation in China. The estimated anomalies for 1640 would tend to reduce the southeasterly moisture flow into the Chinese mainland, and are, therefore, consistent with drier conditions. The estimated sea-level pressure for the dry year of 1640 contrasts with that of the wet year of 1648 (Fig. 8, bottom) when the northern sector of North Pacific subtropical anticyclone is estimated to be intensified, which would encourage moist air flow into eastern China.

Based on the first component of the 44-site precipitation records, 1631 to 1640 is the driest decade and 1881 to 1890, the wettest. The average estimated pressure for 1631 to 1640 (Fig. 9, top) shows lower pressure over most of the grids. This would suggest a weakening of the North Pacific subtropical anticyclone. These results are consistent with the findings of Lough et al. (in preparation) who linked wetter periods in China to an intensified North Pacific subtropical anticyclone and drier conditions to a weakening of this circulation feature. The average estimated sea-level pressure for the wet decade, 1881 to 1890 (Fig. 9, bottom), shows higher pressure estimated over the whole grid with a maximum about 40°N/170°E, indicating an intensification of the North Pacific subtropical anticyclone over this period. The reconstructions developed here appear, therefore, to be reliable though we should note that this test is based on non-independent information—the first principal component of Chinese precipitation being included in the predictor set.

V. CONCLUSIONS

This study has demonstrated how different types of proxy climate records can be combined to give a more reliable estimate of past climate than either record can do individually. The basis for our reconstructions was that both Chinese precipitation variations as recorded in documentary records and western North American tree-ring width variations are influenced by North Pacific sea-level pressure variations. Both sets of predictors calibrate most variance in the vicinity of the North Pacific subtropical anticyclone. The best combined model (CH 44RF+R65TR), calibrated over the period 1899 to 1950 and verified over the independent period 1951 to 1963, explains 44.7% of the summer sea-level pressure variance averaged over the whole grid. Estimates of pressure from this model were derived for each summer season back to 1601. Individually, the Chinese precipitation indices calibrated only 19.7% and the western North American tree-rings 26.0% of the total variance. Although the combined model calibrated variance is not much greater than these, the resulting estimates perform better over the independent verification period.

The guidance of H.C. Fritts is gratefully acknowledged. This work was partially supported by NSF grant ATM-8115754 (H.C. Fritts, principal investigator) from the Climate Dynamics Program of the National Science Foundation and was conducted while Wu Xiangding was a visiting scholar at the Laboratory of Tree-Ring Research.

REFERENCES

Blasing, T.J. (1978), Time series and multivariate analysis in paleoclimatology, In *Time Series and Ecological Processes*, pp. 213—228, H.M. Shugart, Jr., Ed. SIAM-SIMS Conference Series No. 5, Society for Industrial and Applied Mathematics, Philadelphia.

Central Meteorological Bureau (1981), Yearly Charts of Dryness/Wetness in China for the Last 500-Year Period, Cartographic Publishing House, 332 pp.

Fritts, H.C. (1976), Tree Rings and Climate, Academic Press, London, 567 pp.

Fritts, H.C. and Shatz, D.J. (1975), Selecting and characterizing tree-ring chronologies for dendroclimatic analysis *Tree-Ring Bulletin*, **35**: 31—40.

Fritts, H.C. and Lough, J.M. (in press), An estimate of average annual temperature variations for North America, 1602 to 1961, *Climatic Change*.

Fritts, H.C., Lofgren, G.R. and Gordon, G.A. (1979), Variations in climate since 1602 as reconstructed from tree rings, *Quaternary Research*, **12**: 18—46.

Gordon, G.A. (1982), Verification of dendroclimatic reconstructions, In *Climate from Tree Rings*, M.K. Hughes, et al. Eds., Cambridge University Press, Cambridge, pp. 58—61.

Hughes, M.K. et al., Eds. (1982), *Climate from Tree Rings*, Cambridge University Press, Cambridge, 223 pp.

Kutzbach, J.E. and Guetter, P.J. (1980), On the design of paleoenvironmental data networks for estimating large-scale patterns of climate, *Quaternary Research*, **14**:169—187.

Livezey, R.E. and Chen, W.Y. (1983), Statistical field significance and its determination by Monte Carlo techniques, *Mon. Wea. Rev.*, **111**:46—59.

Lofgren, G.R. and Hunt, J.H. (1982), Transfer functions, In Climate from Tree Rings, M.K. Hughes et al. Eds. Cambridge University Press, Cambridge, pp. 50—56.

Lough, J.M. et al. (in preparation), Relationships between the climates of China and North America over the past four centuries: a comparison of proxy records.

National Academy of Sciences (1975), *Understanding Climatic Change*, National Academy Press, Washington, D.C. 239 pp.

Rose, M.R. (1983), Time domain characteristics of tree-ring chronologies and eigenvector amplitude series from western North America. Technical Note No. 25, Laboratory of Tree-Ring Research, University of Arizona, Tucson, Arizona.

Trenberth, K.E. and Paolino, D.A. (1980), The Northern Hemisphere sea-level pressure data set: trends, errors and discontinuities. *Mon. Wea. Rev.* **108**:855—872.

Wang, S. and Zhao, Z. (1981), Drought and floods in China, 1470—1979, In Climate and History, T.M.L. Wigley, et al. Eds., Cambridge University Press, Cambridge, pp. 271—288.